PNAS RESEARCH ARTICLE | ENGINEERING

Invariant dual mechanics of tensegrity and origami

Xiangxin Dang[a] and Glaucio H. Paulino[a,b,1]

Affiliations are included on p. 10.

Edited by Katia Bertoldi, Harvard University, Cambridge, MA; received July 17, 2025; accepted November 25, 2025 by Editorial Board Member Evelyn L. Hu

Statics and kinematics are often viewed as intertwined branches of mechanics. The principle of virtual work indicates this interconnection: For a system in static equilibrium, the total work performed by all forces during any virtual displacement must equal zero. In this work, we make the interplay between statics and kinematics more explicit by focusing on two engineering structures—tensegrity and origami. Specifically, we demonstrate a quantitative duality relationship between the states of self-stress of tensegrity and the infinitesimal mechanisms of origami. More importantly, we show that this duality remains invariant under nondegenerate linear transformations applied to the tensegrity and origami configurations. Furthermore, we establish that the stability property of tensegrity, particularly superstability, is preserved under such transformations. We apply the invariant duality theory to tensegrity and origami structures with prismatic and polyhedral geometries, illustrating its broad applicability. Such duality is also applicable to the fast generation of irregular, three-dimensional architected materials and structures.

duality | invariance | tensegrity | origami

Significance

From termite nests to cancellous bone, irregular structures are ubiquitous in nature but difficult to harness in artificial systems. We propose an optimization-free approach that directly generates irregular structures by applying linear (or, more generally, projective) transformations to regular ones and preserves their mechanical stability or instability throughout the process. This approach reveals the invariance principles underpinning the dual relationship between the statics of tensegrity and the kinematics of origami—two sides of the same coin in structural matrix analysis. Starting from a single regular pair of a self-stressed, superstable tensegrity and a floppy origami, infinite irregular tensegrities and origami mechanisms can be systematically generated, with their static and kinematic characteristics automatically conserved.

Statics and kinematics appear to be intertwined branches of mechanics. Statics is concerned with a balanced system, while kinematics describes the possible motions of a mechanism. The principle of virtual work reveals the inherent interconnection of these two fields—for a system in static equilibrium, the total work done by all forces during any virtual displacement must be zero. The virtual displacements are hypothetical infinitesimal variations of nodal positions that do not violate the geometric constraints of the system. That is to say, the virtual displacements are kinematic in nature. In elasticity, the principle of virtual work directly leads to the fact that the kinematic matrix is the transpose of the equilibrium matrix. In the continuous case, both matrices involve differential operators with respect to the coordinates describing a deformable body. The kinematic matrix relates material point displacements to strains, whereas the equilibrium matrix relates stresses to external body forces. In the discrete case, the matrices are defined by the nodal coordinate differences of members in a pin-jointed framework. The kinematic matrix maps infinitesimal nodal displacements to member elongations, while the equilibrium matrix maps member forces to external nodal forces (1, 2).

When a framework is free-standing, meaning no external nodal forces are applied, the allowable internal forces and nodal displacements are captured within the null spaces of the equilibrium matrix and kinematic matrix, respectively. These null spaces define the states of self-stress or the infinitesimal mechanisms of the framework. In general, a state of self-stress and an infinitesimal mechanism are not necessarily dependent on one another. A framework may exhibit states of self-stress without having any infinitesimal mechanism, or vice versa (2). Interestingly, evidence indicates that certain geometric configurations may establish an equivalence between these two null spaces (3–7). Crapo and Whiteley (3) proved the equivalence between the instantaneous motion of a spherical panel polyhedron and the static stress of the associated bar-and-joint skeleton, under the context of infinitesimal rigidity and static rigidity. Although the concepts of tensegrity and origami were not explicitly stated, the proof in ref. 3 is fundamental for the dual interpretation (in terms of statics and kinematics) of pin-jointed frameworks. Tachi (5) reported a triangulated prismatic framework that can be interpreted either as a self-stressed tensegrity or as infinitesimally foldable (shaky) origami. Here, "tensegrity" (short for "tensional integrity") refers to a framework self-balanced by continuous members in tension (cables) and discontinuous members in compression (struts or bars) (8–11). By this definition, the tensegrity is classified as "class-1," meaning that each node connects to only one strut, ensuring the discontinuity (12). "Origami," on the other hand, refers to a discrete foldable surface (either open or closed) characterized by a set of lines on the surface (creases) where folding occurs (13). In this context, origami is represented

Author contributions: X.D. and G.H.P. designed research; X.D. performed research; X.D. contributed new reagents/analytic tools; X.D. and G.H.P. analyzed data; and X.D. and G.H.P. wrote the paper.

The authors declare no competing interest.

This article is a PNAS Direct Submission. K.B. is a guest editor invited by the Editorial Board.

[1]To whom correspondence may be addressed. Email: gpaulino@princeton.edu.

This article contains supporting information online at https://www.pnas.org/lookup/suppl/doi:10.1073/pnas.2519138123/-/DCSupplemental.

Published March 19, 2026.

by frameworks where members correspond to creases (14). The equivalence lies in the proportionality between the member forces of the tensegrity and the infinitesimal folding angles (i.e., angular velocity) of the origami. Under the scope of origami, this equivalence, or termed "duality," was also demonstrated by Chen and Santangelo (6) for flat, unfolded triangulated networks, and by McInerney et al. (7) for periodic triangulated networks, despite that the concept of tensegrities, particularly those of class-1, was not elucidated. Following these studies, we refer to the equivalent relationship presented in this paper as the duality of tensegrity and origami. The duality provides a clear rationale for why the diagram method (i.e., reciprocal figures), originally developed for calculating balanced forces (15), can also be applied to evaluating first- and second-order flexibility (16).

Origami and tensegrity, beyond their artistic appeal, provide scientific approaches to solving engineering challenges across diverse fields. Origami enables deployable and scalable designs with cutting-edge applications in robotics (17), metamaterials (18), and medical devices (19). Likewise, tensegrity delivers lightweight and deployable systems that have been exploited in biomechanics (20), robotics (21), metamaterials (22), and infrastructure (23). Innovating new origami or tensegrity architectures promises to further broaden their impact across scientific and engineering domains.

The duality of tensegrity and origami suggests a fundamental approach: Origami can draw inspiration from the self-stress analysis of tensegrity, while tensegrity can benefit from insights into the foldability of origami. Mapping from origami to tensegrity poses unique challenges. Simply interpreting folding angle velocities as internal member forces does not guarantee a valid discontinuous distribution of struts or ensure the stability of the resulting tensegrity. Both factors exceed the scope of self-equilibrium described by the duality. The reverse direction, from tensegrity to origami, appears more promising and raises two fundamental questions. First, which tensegrities yield foldable origami? An immediate answer is the prismatic tensegrity and Kresling origami that allow the dual interpretation (Figs. 1 and 2*A*). However, the first question appears to resist a universal solution. We attribute the difficulty to the topological diversity inherent to tensegrity networks. The arrangement of struts and cables can be fairly complex within an arbitrary domain (24). By contrast, an origami structure is locally a two-dimensional discrete manifold partitioned into panels by creases (13). Any tensegrity dual to origami must likewise conform to such manifolds, since duality implies an identical framework geometry for both the tensegrity and the dual origami.

In this paper, we address the second question—given a dual pair of tensegrity and origami, can we exploit that relationship to identify even more dual configurations? We propose invariance theories and show that nondegenerate linear transformations preserve the duality between tensegrity and origami (Figs. 2*B* and 3). Through matrix analysis for pin-jointed frameworks, we prove that such transformations maintain states of self-stress of tensegrity and infinitesimal mechanisms of origami, while analytically quantifying the internal forces, folding angles, and displacements that underpin this duality. In addition, we prove that superstability, the stringent stability condition for tensegrity, is likewise preserved. Based on our theoretical establishments, self-stressed, superstable tensegrity and infinitesimally foldable origami of regular geometry can directly lead to irregular configurations that preserve the equilibrium, superstability, first-order foldability, and the duality. We exemplify all these theories with prismatic geometry and then show their broader applicability with more general polyhedral configurations.

Results

Concept of Duality. Standard prismatic tensegrities (25) and Kresling origami structures (26) have each been well investigated, but largely in isolation. Superficially, both structures exhibit similar geometries—two parallel m-sided polygons twisted and connected by congruent obtuse triangles (Fig. 1, *Left* and *SI Appendix*, Figs. S1 and S2). In tensegrities, only the polygonal and triangular edges exist, as structural members (i.e., cables and struts), whereas origami structures incorporate both faces (polygonal and triangular panels) and edges (creases).

We use α to denote the twist angle of a prismatic tensegrity. The tensegrity is self-stressed, meaning that the internal forces within its members are balanced at each node (Fig. 1, *Top Left*). This static equilibrium reads

$$\sum_{i=1}^{n} F_i \mathbf{n}_i = \mathbf{0}, \qquad [1]$$

where $\mathbf{n}_i$ is the unit direction vector of member i, F_i the magnitude of the corresponding internal force, and n the number of members meeting at each node. Specifically, for the tensegrity in Fig. 1, *Top Left*, $n = 4$. We stipulate that each vector $\mathbf{n}_i$ points away from the node, such that a positive F_i represents tension and a negative F_i represents compression. The direction vectors $\mathbf{n}_i$ depend entirely on the geometry of the tensegrity. Given the dihedral symmetry of standard prismatic tensegrities, Eq. **1** is identical at every node. Then, the unknowns in Eq. **1** become internal forces in the horizontal cables (of length a), the side cables (of length b), and the diagonal struts (of length c), denoted by F_a, F_b, and F_c, respectively (Fig. 1, *Top Left*). For a valid self-stressed configuration guaranteeing solutions to Eq. **1**, the twist angle must satisfy

$$\alpha = \frac{\pi}{2} - \frac{\pi}{m}. \qquad [2]$$

Under the condition of Eq. **2**, solutions to Eq. **1** can be explicitly obtained as $F_a/(-F_c) = a/[2c\sin(\pi/m)]$ and $F_b/(-F_c) = b/c$. We refer to *SI Appendix*, section A for detailed derivations.

We now consider a Kresling origami structure whose geometry matches that of a standard prismatic tensegrity, characterized by creases of lengths a, b, and c, and an undeformed twist angle $\varphi_0 = \alpha$ satisfying Eq. **2**. Consequently, the direction vectors $\mathbf{n}_i$ are identical for both the tensegrity and origami. An infinitesimal mechanism of the origami is a deformation mode preserving kinematic compatibility, i.e., not distorting the panels or tearing the creases. Suppose the mechanism produces infinitesimal dihedral angle variations (or infinitesimal folding angles), $\mathrm{d}\theta_i$ (Fig. 1, *Bottom Left*). Then, the kinematic compatibility, that any panel rotates by zero degree with respect to itself throughout a loop of relative rotations, is expressed as

$$\sum_{i=1}^{n} \mathrm{d}\theta_i \mathbf{n}_i = \mathbf{0}. \qquad [3]$$

By comparing Eqs. **1** and **3**, we find that F_i in the tensegrity and $\mathrm{d}\theta_i$ in the origami satisfy identical equations. Analogous to tension and compression in tensegrity members, a positive

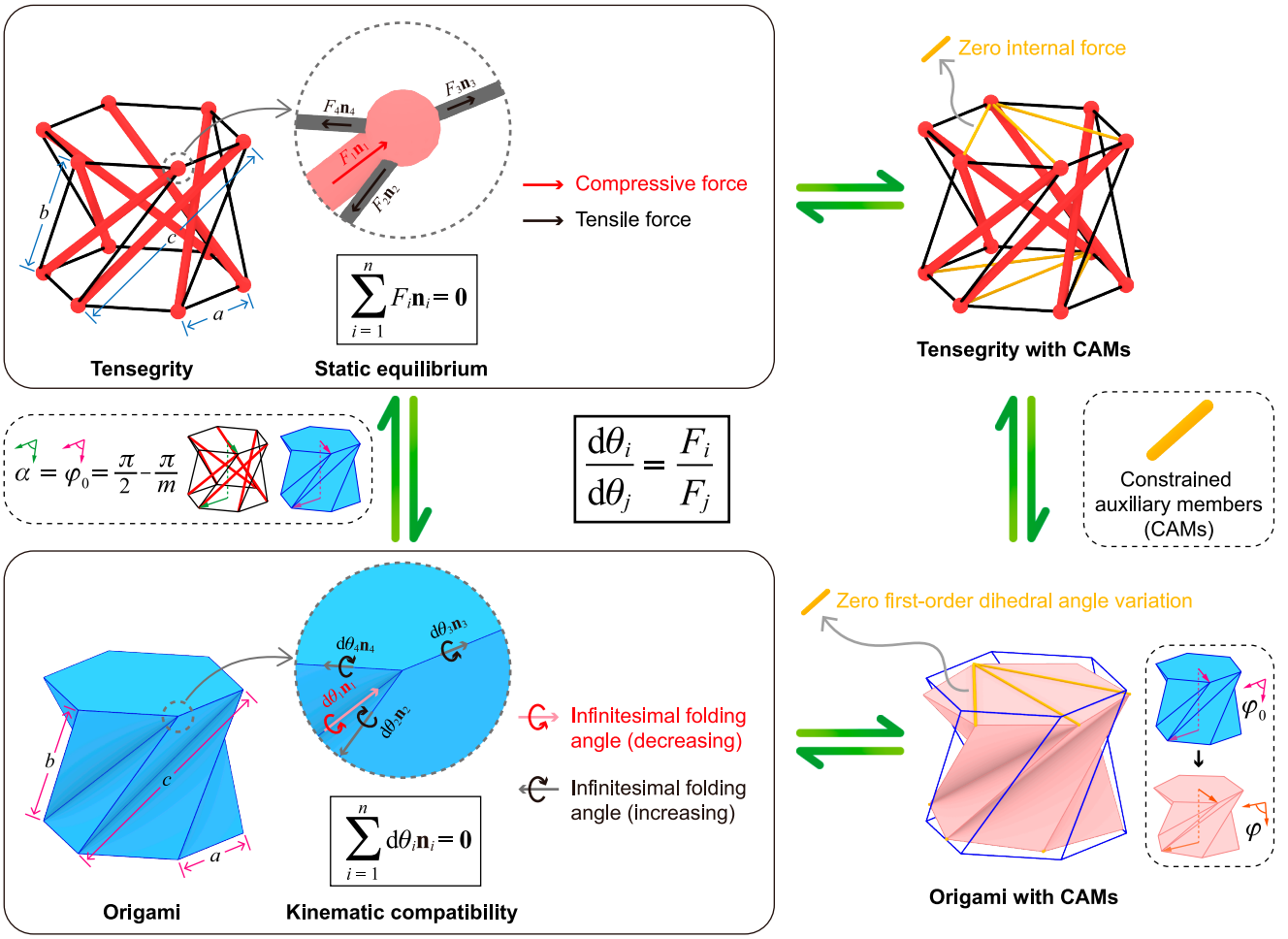

Fig. 1. Duality of tensegrity and origami. The static equilibrium of self-stressed tensegrity and the kinematic compatibility of shaky origami are controlled by identical linear equations for the internal forces F_i and the infinitesimal folding angles $\mathrm{d}\theta_i$, respectively. These equations reveal the proportional duality relationship $\mathrm{d}\theta_i/\mathrm{d}\theta_j = F_i/F_j$, provided that the tensegrity and origami possess the same triangulated framework geometry forming the outline of a polyhedron. For the prismatic configurations, the existence of such self-equilibrium and infinitesimal mechanism requires that the twist angle between the two base polygons (denoted by α for the tensegrity and by φ_0 for the origami) is $\pi/2 - \pi/m$, where m is the number of sides for each polygon. The infinitesimal deformation twists the prismatic (Kresling) origami from φ_0 to φ.

$\mathrm{d}\theta_i$ indicates an increasing dihedral angle, while a negative $\mathrm{d}\theta_i$ indicates a decreasing dihedral angle. Thus, Eq. **3** shares the same solutions as Eq. **1**. Since both are linear equations, their solutions satisfy

$$\frac{\mathrm{d}\theta_i}{\mathrm{d}\theta_j} = \frac{F_i}{F_j}, \qquad [4]$$

where indices i, j represent two members in the tensegrity and two corresponding creases in the origami. Generally, suppose the rank of the linear equation system (defined by either Eq. **1** or Eq. **3**) is r_{LES}, then Eq. **4** must have r_{LES} branches corresponding to r_{LES} sets of linearly independent solutions. For the prismatic configurations, $r_{\mathrm{LES}} = 1$. For the specific prismatic geometry, Eq. **4** becomes $\mathrm{d}\theta_a : \mathrm{d}\theta_b : \mathrm{d}\theta_c = F_a : F_b : F_c$, where $\mathrm{d}\theta_a$, $\mathrm{d}\theta_b$, and $\mathrm{d}\theta_c$ are infinitesimal folding angles at the horizontal creases (of length a), the side creases (of length b), and the diagonal creases (of length c), respectively. These infinitesimal folding angles can also be directly derived through folding kinematics analysis (*SI Appendix*, section B), yielding $\mathrm{d}\theta_a = a/[2h\sin(\pi/m)]\mathrm{d}\varphi$, $\mathrm{d}\theta_b = (b/h)\mathrm{d}\varphi$, and $\mathrm{d}\theta_c = (-c/h)\mathrm{d}\varphi$. Here, $\mathrm{d}\varphi$ is an infinitesimal change of the twist angle φ away from its initial value $\varphi_0 = \alpha$, and h the height of the Kresling origami (or equivalently, the height of the prismatic tensegrity).

Remarkably, using the duality relationship of Eq. **4**, we have directly determined the ratios of infinitesimal folding angles in an origami structure based solely on known states of self-stress of the corresponding tensegrity, thereby avoiding any kinematics analysis. Also, we do not need to solve Eq. **3** again because we have solved the same Eq. **1** for the tensegrity.

Notably, the kinematic compatibility of Eq. **3** relies on the closed configurations of the origami structures. For example, in Fig. 1, *Bottom Left*, if the hexagonal panels were absent, the angular differentials $\mathrm{d}\theta_3\mathbf{n}_3$ and $\mathrm{d}\theta_4\mathbf{n}_4$ could not be defined, consequently invalidating the duality of Eq. **4**. Thus, the duality relationship exists only when the origami form a closed shape, i.e., a polyhedron whose boundary is topologically equivalent to a sphere. The Kresling origami presented in this work, despite their prismatic geometry, are indeed polyhedral, enclosed by the *Top* and *Bottom* polygons and the side triangles. We refer to *SI Appendix*, Fig. S3 for more prismatic configurations with different numbers of polygon sides.

Framework Interpretation. In a unified treatment, a tensegrity and its dual origami structure can be regarded as the same free-standing pin-jointed framework that forms the skeleton of a polyhedron. The geometry (i.e., nodal coordinates and member

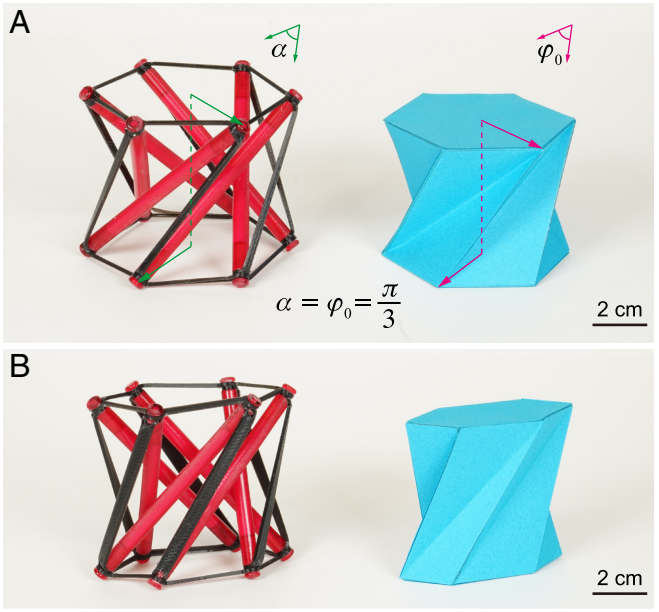

Fig. 2. Prototypes of dual tensegrities and origami structures. (*A*) Regular prismatic configurations. (*B*) Irregular prismatic configurations obtained through a linear transformation (combining stretching and shear) applied to the regular configurations.

connectivity) of the framework defines its kinematic matrix $\mathbf{B}$ and equilibrium matrix $\mathbf{D}$, with $\mathbf{B}^{\mathrm{T}} = \mathbf{D}$. Then, the member force vector $\mathbf{s}$ of the self-stressed tensegrity satisfies $\mathbf{Ds} = \mathbf{0}$, and the infinitesimal nodal displacement vector $\mathbf{m}$ of the shaky origami structure satisfies $\mathbf{Bm} = \mathbf{0}$. The infinitesimal folding angle vector $\mathrm{d}\boldsymbol{\theta}$ can be expressed as $\mathrm{d}\boldsymbol{\theta} = \mathbf{Jm}$, where $\mathbf{J}$ is the Jacobian matrix of dihedral angles with respect to nodal coordinates. The above process is detailed in *SI Appendix*, sections C.2–C.4. In this setting, the duality of Eq. **4** can be rewritten in the compact form as

$$\mathbf{s} = \mu\mathbf{Jm}, \qquad [5]$$

where μ is an arbitrary nonzero coefficient with the unit of N. From the practical perspective, this reformulation is crucial as Eq. **5** involves the explicit description of kinematics with the mechanism displacements (components of $\mathbf{m}$), bridging the gap from the inexplicit description with dihedral angle variations (components of $\mathrm{d}\boldsymbol{\theta}$). The Jacobian $\mathbf{J}$ is explicitly determined by the geometry, i.e., nodal coordinates and member connectivity of a framework (14). Thus, the duality of Eq. **5** captures the intrinsic relationship between statics (described by $\mathbf{s}$) and kinematics (described by $\mathbf{m}$) that arises purely from the framework geometry, independent of material properties.

Importantly, performing the above framework analysis requires triangulating the polyhedron by adding constrained auxiliary members over diagonals of its polygonal faces (Fig. 1, *Right*). These auxiliary members are constrained in the sense that they carry zero internal force in the tensegrity's state of self-stress and exhibit zero first-order dihedral angle variation (as well as zero first-order elongation) in the origami's mechanism deformation mode, which merges into the dual relationships. In other words, the added members do not affect the self-balance of the tensegrity and avoid the distortion of the polygonal panels of the origami. In addition, they facilitate calculating $\mathrm{d}\boldsymbol{\theta}$ from $\mathbf{m}$ based on the triangulation scheme (*SI Appendix*, Fig. S4). Remarkably, the triangulation not only serves as a technical implementation but also discloses the fundamental rationale that underpins the duality relationship. To explain this, we let d_m denote the number of independent infinitesimal mechanisms and d_s denote the number of independent states of self-stress, of the same triangulated pin-jointed framework. Hence, the null space of $\mathbf{B}$ is $(d_m + 6)$-dimensional (considering six rigid body motion modes) and the null space of $\mathbf{D}$ is d_s-dimensional. Suppose the framework consists of N nodes and M edges (cables and struts for tensegrity or creases for origami), and the triangulated polyhedron has F faces. The general Maxwell relation (2) gives $d_s - (d_m + 6) = M - 3N$. The triangulation implies $3F = 2M$. Furthermore, for any polyhedron that is homeomorphic to a sphere, the Euler characteristic is a constant: $\chi = N - M + F = 2$. These three equations yield an important result: $d_s = d_m$, which reveals the coexistence of the infinitesimal mechanisms $\mathbf{m}$ and the states of self-stress $\mathbf{s}$ of a triangulated polyhedral framework. This provides the theoretical foundation for the duality relationship of Eq. **5** beneath the geometric identity between tensegrity and origami. For the prismatic configurations, we have $d_s = d_m = 1$, equivalent to $r_{\mathrm{LES}} = 1$ when the constraints of auxiliary members are applied. As McInerney et al. (7) pointed out, periodic origami sheets that are extended indefinitely in space also admit dual states of self-stress and folding modes, such as triangulations of Miura-ori and eggbox sheets ($d_s = d_m = 3$), and cylindrical origami sheets ($d_s = d_m = 2$). Moreover, the case of $d_s = d_m = 0$ is closely related to the well-known Cauchy's theorem (27) and its associated result in rigidity theory that convex triangulated polyhedra are isostatic (not supporting a stress), as mentioned in refs. 3 and 28. Therefore, the nonconvexity of the prismatic configurations (i.e., the existence of valleys) that we present is also in essence for the emergence of static and kinematic indeterminacy in the duality relationship.

Linear Transformation. Let $\mathbf{T}$ be a three-dimensional linear transformation applied to the nodal coordinates of a framework representing a tensegrity and its dual origami. This work is focused on spatial structures and therefore we stipulate that $\mathbf{T}$ is nondegenerate. Technically, the nondegeneracy avoids collapsing the framework down into lower-dimension (i.e., a plane, line, or point), where member self-intersections may occur. To distinguish the frameworks before and after the transformation $\mathbf{T}$, we use the following definition:

Definition 1: A new free-standing pin-jointed framework is obtained by applying a nondegenerate three-dimensional linear transformation $\mathbf{T}$ to the nodal coordinates $\mathbf{r}_k = [x_k, y_k, z_k]^{\mathrm{T}}$ ($k = 1, 2, \ldots, N$) of an old three-dimensional free-standing pin-jointed framework.

The effect of $\mathbf{T}$ is intuitive if we define $\mathbf{l}_i = \ell_i\mathbf{n}_i$ and rewrite Eqs. **1** and **3** as $\sum_{i=1}^{n}(F_i/\ell_i)\mathbf{l}_i = \mathbf{0}$ and $\sum_{i=1}^{n}(\mathrm{d}\theta_i/\ell_i)\mathbf{l}_i = \mathbf{0}$, respectively. Here, $\mathbf{l}_i$ are direction vectors of the members, and their coefficients become the force densities F_i/ℓ_i and the folding angle densities $\mathrm{d}\theta_i/\ell_i$. Obviously, these coefficients are exactly the solutions of $\sum_{i=1}^{n}(F_i/\ell_i)\mathbf{T}\mathbf{l}_i = \mathbf{0}$ and $\sum_{i=1}^{n}(\mathrm{d}\theta_i/\ell_i)\mathbf{T}\mathbf{l}_i = \mathbf{0}$. We use the tilde symbol to mark the physical quantities ($\tilde{\ell}_i$, $\tilde{F}_i$, $\mathrm{d}\tilde{\theta}_i$, $\tilde{\mathbf{l}}_i$, etc) for the new framework. Then, we have the new equilibrium and compatibility equations $\sum_{i=1}^{n}(\tilde{F}_i/\tilde{\ell}_i)\tilde{\mathbf{l}}_i = \mathbf{0}$ and $\sum_{i=1}^{n}(\mathrm{d}\tilde{\theta}_i/\tilde{\ell}_i)\tilde{\mathbf{l}}_i = \mathbf{0}$, respectively. Since $\tilde{\mathbf{l}}_i = \mathbf{T}\mathbf{l}_i$, the invariance of force densities $\tilde{F}_i/\tilde{\ell}_i = F_i/\ell_i$ and the invariance of folding angle densities $\mathrm{d}\tilde{\theta}_i/\tilde{\ell}_i = \mathrm{d}\theta_i/\ell_i$ are immediately revealed. While this observation is trivial for some transformations (e.g., dilation, rotation, and reflection), it predicts the coexistence

of infinitesimal mechanisms and states of self-stress for irregular frameworks (with less symmetries) generated through shear and stretching (*SI Appendix*, Fig. S5).

Invariance of Duality. Beyond the intuitive analysis, it is important to incorporate the infinitesimal nodal displacements ($\mathrm{d}\mathbf{r}_k$ in $\mathbf{m}$ and $\mathrm{d}\tilde{\mathbf{r}}_k$ in $\tilde{\mathbf{m}}$) for explicitly describing the kinematics, dual to the statics (F_i in $\mathbf{s}$ and $\tilde{F}_i$ in $\tilde{\mathbf{s}}$). This development relies on the fact that the new framework inherits the coexistence of $\mathbf{m}$ and $\mathbf{s}$, expressed by $\tilde{d}_s = \tilde{d}_m = d_s = d_m$ (*SI Appendix*, section D and Lemma 1). Matrix analysis leads to the following two theorems (*SI Appendix*, section D and Theorems 1 and 2):

Theorem 1 (tensegrity: invariance of equilibrium). *If the old framework has a state of self-stress with internal forces F_i ($i = 1, 2, ..., M$), then the new framework must have a state of self-stress with internal forces $\tilde{F}_i = (\tilde{\ell}_i/\ell_i)F_i$ ($i = 1, 2, ..., M$).*

Theorem 2 (origami: invariance of infinitesimal mechanism). *If the old framework has an infinitesimal mechanism with displacements $d\mathbf{r}_k = [dx_k, dy_k, dz_k]^T$ ($k = 1, 2, ..., N$) and dihedral angle variations $d\theta_j$ ($j = 1, 2, ..., M$), then the new framework must have an infinitesimal mechanism with displacements $d\tilde{\mathbf{r}}_k = det(\mathbf{T})\mathbf{T}^{-T}d\mathbf{r}_k$ and dihedral angle variations $d\tilde{\theta}_j = (\tilde{\ell}_j/\ell_j)d\theta_j$.*

Theorem 2 indicates that the new nodal displacements $\det(\mathbf{T})\mathbf{T}^{-\mathrm{T}}\mathrm{d}\mathbf{r}_k$ are explicitly determined by $\mathbf{T}$ and the old displacements $\mathrm{d}\mathbf{r}_k$. This specific form is reminiscent of the cross product identity $(\mathbf{T}\mathbf{l}_i) \times (\mathbf{T}\mathbf{l}_j) = \det(\mathbf{T})\mathbf{T}^{-\mathrm{T}}(\mathbf{l}_i \times \mathbf{l}_j)$, where $(\mathbf{T}\mathbf{l}_i) \times (\mathbf{T}\mathbf{l}_j)$ and $\mathbf{l}_i \times \mathbf{l}_j$ represent the new and old panel normals, respectively, for the edge direction vectors $\mathbf{l}_i$ and $\mathbf{l}_j$ of the origami. This form similarity between new nodal displacements and new panel normals is the basis of the folding angle density invariance $\mathrm{d}\tilde{\theta}_j/\tilde{\ell}_j = \mathrm{d}\theta_j/\ell_j$, since the panel orientations and the nodal displacements collectively determine the dihedral angle changes between two panels (*SI Appendix*, section D and Theorem 2).

Considering Eq. **4**, *Theorems* 1 and 2 directly lead to the new duality relationship:

$$\frac{\mathrm{d}\tilde{\theta}_i}{\mathrm{d}\tilde{\theta}_j} = \frac{\tilde{F}_i}{\tilde{F}_j}. \qquad [6]$$

Eq. **6** is trivial because the duality (arising from Eqs. **1** and **3**) is a universal rule for both regular and irregular frameworks that are skeletons of polyhedra. The compact form is less intuitive, which involves the new infinitesimal nodal displacement vector $\tilde{\mathbf{m}} = \det(\mathbf{T})\mathbf{T}_{3N}^{-\mathrm{T}}\mathbf{m}$ and the new member force vector $\tilde{\mathbf{s}} = \tilde{\mathbf{L}}\mathbf{L}^{-1}\mathbf{s}$. Here, $\mathbf{T}_{3N}$ is the high-dimensional ($3N$-by-$3N$) version of $\mathbf{T}$ (see its definition in *SI Appendix*, section C.1). They are connected by the new Jacobian $\tilde{\mathbf{J}}$ as

$$\tilde{\mathbf{L}}\mathbf{L}^{-1}\mathbf{s} = \mu\tilde{\mathbf{J}}[\det(\mathbf{T})\mathbf{T}_{3N}^{-\mathrm{T}}\mathbf{m}], \qquad [7]$$

where $\tilde{\mathbf{L}}$ and $\mathbf{L}$ are the diagonal matrices whose nonzero components are $\tilde{l}_i$ and l_i, respectively. Notice that Eqs. **5** and **7** share the same coefficient μ. This means that each pair of $\mathbf{m}$ and $\mathbf{s}$ for the old framework must correspond to a dual pair of $\tilde{\mathbf{m}}$ and $\tilde{\mathbf{s}}$ for the new framework satisfying an invariant proportional relationship.

With *Theorems* 1 and 2, we can directly compute the internal forces of an irregular tensegrity and the infinitesimal mechanism displacements of an irregular origami structure if the irregular geometry is generated by applying a linear transformation to a regular structure whose equilibrium or kinematics is already known. For example, Fig. 3 illustrates the regular and irregular prismatic tensegrities and Kresling origami structures under $\mathbf{T} = \mathbf{S}_{xy}\mathbf{S}_z$. Here, $\mathbf{S}_{xy}$ is a simple shear in the xy-plane and $\mathbf{S}_z$ is a stretching in the z-direction (*SI Appendix*, Fig. S5). We recall the internal force relationship for the regular prismatic tensegrity: $F_a/(-F_c) = a/[2c\sin(\pi/m)]$ and $F_b/(-F_c) = b/c$. Specifically, when $m = 6$, we have $F_a/a = F_b/b = -F_c/c$. Then, *Theorem* 1 immediately suggests that the irregular tensegrity in Fig. 3, *Left* has uniform force densities $\tilde{F}_i/\tilde{\ell}_i$ across all the members (negative values for the struts and positive values for the cables, with the same magnitude). The duality of Eq. **6** indicates that the corresponding irregular origami also has uniform folding angle densities $\mathrm{d}\tilde{\theta}_i/\tilde{\ell}_i$. Moreover, *Theorem* 2 predicts the irregular infinitesimal mechanism mode, which is a twisting mode similar to that of the regular Kresling origami (Fig. 3, *Right*). The combined effects of $\mathbf{T}$ (to the configuration geometry by $\tilde{\mathbf{r}}_k = \mathbf{T}\mathbf{r}_k$) and $\mathbf{T}^{-\mathrm{T}}$ (to the nodal displacements by $\mathrm{d}\tilde{\mathbf{r}}_k = \det(\mathbf{T})\mathbf{T}^{-\mathrm{T}}\mathrm{d}\mathbf{r}_k$) finally produce similar deformation modes, i.e., $\mathrm{d}\mathbf{r}_k$ at $\mathbf{r}_k$ versus $\mathrm{d}\tilde{\mathbf{r}}_k$ at $\tilde{\mathbf{r}}_k$.

We perform twisting simulations to obtain the finite nodal displacements of the regular Kresling origami (denoted by $\mathbf{d}_k$ for node k) under the principle of minimum potential energy (Fig. 4*A*). Both the nondimensional energy $U/(EAL)$ and the maximum edge strain $|\varepsilon|_{\max}$ have zero slope at the initial deformation regime (yellow curves in Fig. 4 *B* and *C* for the configuration with hexagons; see *SI Appendix*, Fig. S3 *B* and *C* for more configurations), indicating the mechanism deformation. Then, we estimate the irregular nodal displacements $\tilde{\mathbf{d}}_k$ by directly applying *Theorem* 2 to the finite displacements $\mathbf{d}_k$. This development yields possible deformation paths of the irregular Kresling origami generated through the transformation $\mathbf{T}$, which is either a stretching ($\mathbf{S}_x$, $\mathbf{S}_y$, $\mathbf{S}_z$), a shear ($\mathbf{S}_{xy}$, $\mathbf{S}_{yz}$, $\mathbf{S}_{zx}$), or their combinations ($\mathbf{S}_{xy}\mathbf{S}_z$, etc). These irregular configurations are shown in *SI Appendix*, Fig. S5. Their estimated curves of $U/(EAL)$ and $|\varepsilon|_{\max}$ (Fig. 4 *B* and *C*) all have zero slope at the initial deformation regime. Since the real paths (satisfying the principle of minimum potential energy) must have lower energy than the possible paths, the real slopes must be zero as well, indicating the infinitesimal mechanisms of the irregular configurations. Although the regular structure twists until its side faces collide (Fig. 4*A*), edge contact is observed in the irregular structures (particularly, those transformed by $\mathbf{S}_{xy}$, $\mathbf{S}_{xy}\mathbf{S}_y$, and $\mathbf{S}_{xy}\mathbf{S}_z$, as shown in Fig. 4 *B* and *C*). While the simple shear ($\mathbf{S}_{xy}$, $\mathbf{S}_{yz}$, and $\mathbf{S}_{zx}$, as shown in Fig. 4 *B* and *C*) tend to make the irregular structures collide at the early deformation stage ($\varphi_1 < 30°$), the combination of simple shear and stretching could mitigate this effect. This analysis suggests a strategy for the fast approximation of irregular structural deformations (Movie S1).

Tensegrity Stability. Self-equilibrium, preserved by the nondegenerate linear transformation $\mathbf{T}$, does not guarantee structural integrity if the stability property is not taken into account. Here, we show that $\mathbf{T}$ also preserves the stability of a tensegrity. We are particularly interested in tensegrities which are always stable regardless of member materials and levels of prestress, namely superstability. The superstability is closely related to the force density matrix $\mathbf{E}$ and the geometry matrix $\mathbf{G}$, where $\mathbf{E}$ defines the self-equilibrium, and $\mathbf{G}$ describes the nontrivial affine motions. Specifically, a superstable tensegrity must have a full rank $\mathbf{G}$ and a positive semidefinite $\mathbf{E}$. Under these two necessary

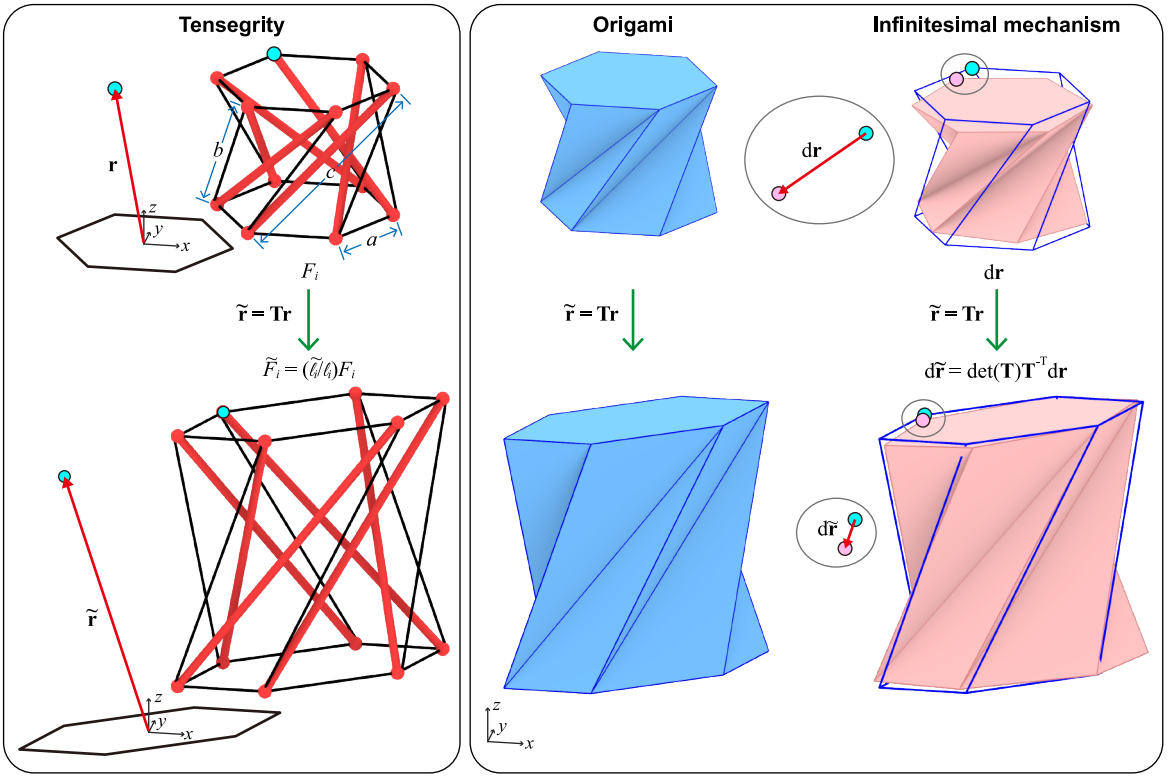

Fig. 3. Invariance of tensegrity self-equilibrium and origami infinitesimal mechanism under the nondegenerate linear transformation **T**. Here, $\mathbf{T} = \mathbf{S}_{xy}\mathbf{S}_z$, in which $\mathbf{S}_{xy}$ is a simple shear in the *xy*-plane and $\mathbf{S}_z$ is a stretching in the *z*-direction. The new nodal coordinates $\tilde{\mathbf{r}}$, internal forces $\tilde{F}_i$, nodal displacements $d\tilde{\mathbf{r}}$ are determined by the old geometry and the transformation **T**.

conditions, if the rank deficiency of **E** is four, any infinitesimal mechanism of a pin-jointed framework is resisted by its internal forces (prestress), guaranteeing the superstability (*SI Appendix*, section C.5). We have shown the invariance of force densities $\tilde{F}_i/\tilde{\ell}_i = F_i/\ell_i$, which means that **T** does not change the rank or the positive semidefiniteness of **E**. In addition, **T** does not change the rank of **G** (*SI Appendix*, section D and Lemma 2). Then, the superstability of the new tensegrity becomes a natural result (*SI Appendix*, section D and Theorem 3):

Theorem 3 (tensegrity: invariance of superstability). *If the old framework is superstable and its force density matrix* **E** *is of rank deficiency four, then the new framework must be superstable.*

For example, since the regular prismatic tensegrities are superstable and their force density matrices have rank deficiency of four (as proved in ref. 9), *Theorem* 3 instantly indicates that all their irregular variants under **T** (e.g., those in *SI Appendix*, Fig. S5) are also superstable. This is a strong result that benefits the design and fabrication of irregular tensegrities as superstability relaxes the requirement of levels of prestress and constituent materials.

Nonlinear Transformation. It is noteworthy that nonlinear transformations may either disrupt or preserve the self-equilibrium of a tensegrity or the internal mechanism of an origami. To show this, first, we apply a gradient rotation (no rotation to the bottom face and a finite rotation to the top face) to the Kresling origami with an infinitesimal mechanism mode (Fig. 5*A*). The outcome is a different Kresling origami structure that loses the mechanism mode—although both origami structures have zero variation rate of $U/(EAL)$ initially (Fig. 5*B*), the one after the gradient rotation (which is a nonlinear transformation) shows nonzero variation rate of $|\varepsilon|_{\max}$. In fact, we have assigned the specific rotation angle to the top face so that the new Kresling origami structure is bistable, which is not dual to any tensegrity.

Second, linear transformations are not the only class of geometric transformations that preserve the duality relationship. In fact, projective transformations (a broader class that includes linear transformations) also leave the statics and kinematics of a pin-jointed framework unaltered. The relevant literature dates back to Rankine (29), and this fact was proven by Crapo and Whiteley (3). As the proof in ref. 3 was made extremely concise under the projective geometry setting, we provide an alternative derivation with detailed steps in *SI Appendix*, section F. Fig. 6 shows two examples that nonlinear projective transformations are applied to the regular Kresling origami and tensegrity, generating new dual pairs of tensegrity and shaky origami. More details about the projection direction **h** and the projective transformations used to generate these two examples are given in *SI Appendix*, section F. After applying the projective transformations, the parallel lines associated with the original prismatic configuration intersect at a common point, if these parallel lines are not perpendicular to the projection direction. Particularly, the conical shaky origami in Fig. 6*A* and its bistable variants were analytically investigated in ref. 30. By contrast, the tensegrity and origami in Fig. 6*B* exhibits less symmetry, but their static and kinematic indeterminacy are obvious with the aid of projective transformations.

We note a crucial distinction between a general nonlinear projective transformation (preserving incidence but with perspective) and a linear transformation (preserving both incidence and parallelism): The perspective may alter the class number

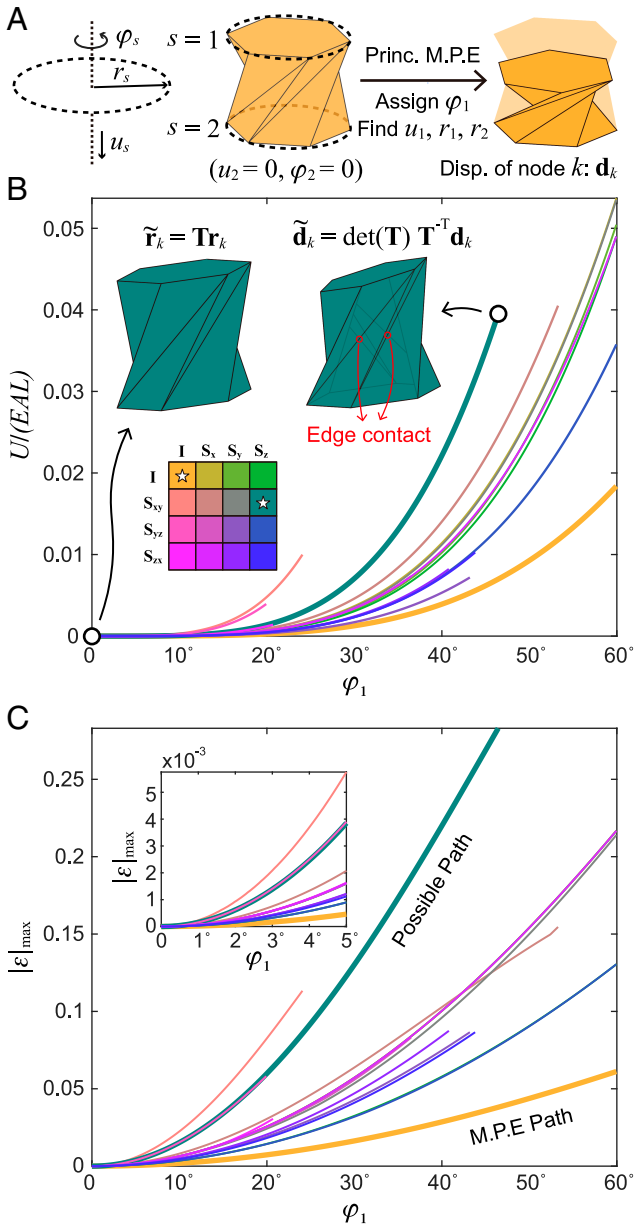

Fig. 4. Finite deformation simulation and approximation of shaky prismatic origami. (*A*) The finite nodal displacements $\mathbf{d}_k$ at the nodes $\mathbf{r}_k$ of the regular prismatic origami are simulated under the principle of minimum potential energy. Leveraging the configuration symmetry, the twist angles φ_s, circumferential radii r_s, and the translations u_s of the two base polygons ($s = 1, 2$) define the overall deformation, with $u_2 = 0$ and $\varphi_2 = 0$ restricting the rigid-body motion. In the simulation, we use the pin-jointed framework model in which the deformation energy U is stored in the members, and all the members are assumed to have the same elastic modulus E and cross-sectional area A. (*B*) The nondimensional energy $U/(EAL)$ and (*C*) the maximum edge strain $|\varepsilon|_{\max}$ of the origami obtained through $\mathbf{T}$. Here, L is the length of any valley crease on the undeformed regular structure. As illustrated by the color map, $\mathbf{T}$ can be an identity ($\mathbf{I}$), a stretching ($\mathbf{S}_x$, $\mathbf{S}_y$, $\mathbf{S}_z$), a shear ($\mathbf{S}_{xy}$, $\mathbf{S}_{yz}$, $\mathbf{S}_{zx}$), and their combinations ($\mathbf{S}_{xy}\mathbf{S}_z$, etc). For the irregular origami ($\mathbf{T} \neq \mathbf{I}$), the finite nodal displacements are approximated with the linear formulation $\tilde{\mathbf{d}}_k = \det(\mathbf{T})\mathbf{T}^{-\mathrm{T}}\mathbf{d}_k$, yielding possible deformation paths that are used to generate the curves. The curves end either when face contact or edge contact (edge-face intersection) occurs, or at the twist angle $\varphi_1 = 60°$ corresponding to the final state of the regular structure.

of a tensegrity or cause physically invalid result (*SI Appendix*, section F). Thus, nonlinear projective transformations introduce additional complication compared to the linear transformations. Although the projective (including the linear) invariance and the duality are not limited to class-1 tensegrities, in practice, class-1 tensegrities are elegant (from a structural point of view) and of special interest in regard to manufacturing (12). With linear transformations, the class number of tensegrities is desirably preserved.

Moreover, regarding the invariance of superstability of tensegrities, the proof of *Theorem* 3 involves the fact that the rank and the positive semidefiniteness of the force density matrix remain unchanged under linear transformations. This property was presented in a more general form by Connelly and Whiteley (31), and was also mentioned by Connelly and Terrel (32): Projective transformations do not change the signature (the numbers of positive, negative, and zero eigenvalues) of the stress matrix (another term for the force density matrix). However, this general conclusion holds only when no node is sent to infinity. Otherwise, the members associated to nodes at infinity must carry zero internal force, which may in turn alter the signature of the force density matrix.

More Polyhedral Configurations. Our invariant dual theories provide systematic answers to the second question we have asked—given a dual pair of tensegrity and origami, one can generate infinitely more dual configurations simply via linear transformations. Moreover, the statics (i.e., internal forces) and the infinitesimal mechanisms (i.e., dihedral angle variations and nodal displacements) are explicitly expressed for the generated configurations. Regarding the first question, we have shown the prismatic tensegrities that lead to shaky Kresling origami. Although referred to as "prismatic" configurations, the origami are essentially closed polyhedra and the tensegrities form skeletons of these polyhedra. Here, we show more polyhedral configurations that allow the dual interpretation. The idea comes from Snelson's six-bar icosahedral tensegrity (33) and Jessen's orthogonal icosahedron (34), that exhibit identical geometry. The icosahedral tensegrity belongs to the rhombic truncated regular polyhedral (TRP) tensegrities (35), whose truncated tetrahedral, cubic, and dodecahedral configurations are formed by replicating rhombic cells with one strut and two types of cables (*SI Appendix*, Fig. S6). By tuning force densities in the strut and cables, one can obtain various superstable rhombic TRP tensegrities (*SI Appendix*, section E). These tensegrities

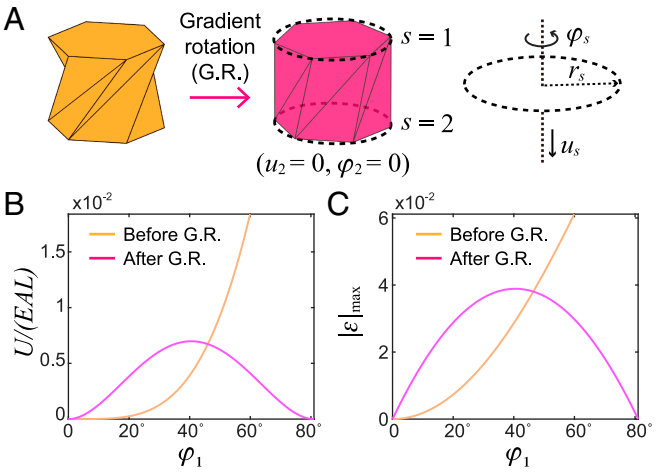

Fig. 5. Finite deformation simulation of two prismatic origami structures whose configurations are transformed through a gradient rotation. (*A*) The old and new origami configurations with a finite rotation to the top face and no rotation to the bottom face. (*B*) The nondimensional energy $U/(EAL)$ and (*C*) the maximum edge strain $|\varepsilon|_{\max}$ of the two origami structures.

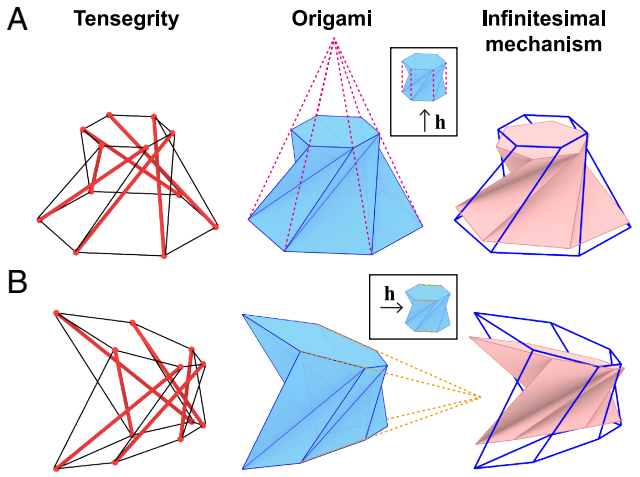

Fig. 6. Irregular tensegrities (*Left* Column), the dual origami (*Middle* Column), and the infinitesimal mechanisms (*Right* Column) generated by applying nonlinear projective transformations to the regular prismatic configuration (shown in *Insets*). (*A*) The projection direction **h** is perpendicular to the base polygons. (*B*) The projection direction **h** is parallel to the base polygons. Unlike linear transformations, nonlinear projective transformations do not preserve parallelism (see the dashed lines).

unveil the corresponding shaky origami structures as a result of duality (*SI Appendix*, Fig. S7). Particularly, one can specify force densities such that the two types of cables have the same length, generating regular tensegrity and origami configurations (Fig. 7, *Left* and *Middle* and *SI Appendix*, Fig. S7, *Bottom*). The infinitesimal mechanisms of these origami structures are uniform contractions (Fig. 7, *Right*), validated by numerical simulations (*SI Appendix*, Fig. S8 and Movie S1). The contractions are driven by the local twisting of the rhombic cells that also appear in Kresling origami (*SI Appendix*, Fig. S9). According to *Theorems* 1–3, a nondegenerate linear transformation $\mathbf{T}$ generates irregular superstable tensegrities and irregular shaky origami that maintain the dual relationships (*SI Appendix*, Figs. S10–S12). The estimated $U/(EAL)$ and $|\varepsilon|_{\max}$ demonstrate zero initial slopes, validating the infinitesimal mechanisms of these irregular origami structures (*SI Appendix*, Fig. S13).

Discussion

We have presented the duality of tensegrity and origami and the invariance of static equilibrium, infinitesimal mechanism kinematics, and superstability under nondegenerate linear transformations applied to such dual configurations. Although we have illustrated tensegrities with one independent state of self-stress and origami with one independent infinitesimal mechanism ($d_s = d_m = 1$), the invariant dual mechanics holds generally for any $d_s = d_m \geq 1$. For example, Fig. 8 presents various three-layer prismatic configurations exhibiting either $d_s = d_m = 1$ or $d_s = d_m = 3$. Specifically, the $d_s = 1$ tensegrity (Fig. 8*A*) is class-1, with its connectivity and nodal-coordinate formulations available in refs. 25 and 36. By contrast, the $d_s = 3$ tensegrity (Fig. 8*B*) is class-2, where each independent self-stress state corresponds to a replication of a single one-layer prismatic tensegrity, dual to the corresponding independent infinitesimal mechanism of the origami tower (Fig. 8 *C* and *D*). A nondegenerate linear transformation preserves not only the number of independent self-stress states and infinitesimal mechanisms, but also the tensegrity class (Fig. 8 *E*–*H*). The concept of duality bridges stable and shaky structures and enables the discovery of one based on prior knowledge of the other. The invariance theories reveal an optimization-free approach for the fast generation of three-dimensional irregular structures with preserved static or kinematic properties. Such optimization-free design principle of explicitly transforming nodal coordinates has been appreciated in two-dimensional shape-morphing kirigami systems (37). Our invariance theories pave the way for designing three-dimensional architected materials by assembling irregular building blocks, provided that the assembly process is facilitated by proper connection rules (38). Finally, as there exist finitely flexible polyhedra (39), the invariant dual mechanics is potentially generalizable beyond infinitesimal mechanisms to include finite isometric deformations. One of the challenges is to investigate how the linear transformation, which is known only for the initial configuration in the current theory, would evolve on the finite kinematic path of the origami structures. If the transformation, and even its inverse (which appears in the displacement formulation), can be analytically expressed, it would be possible to integrate the entire system (the differentials of the folding motion and the transformation) to approximate the finite motion of the transformed structures. With the duality relationship, these findings for finitely foldable origami structures could be directly mapped to tensegrities that are to be discovered.

Materials and Methods

Simulation. We build a surrogate model to capture the finite deformations of the regular origami structures (i.e., those before the transformation $\mathbf{T}$). We adopt the framework interpretation and assume that the deformation energy is stored in the framework members (including the constrained auxiliary members). As shown in Figs. 4*A* and 5*A*, we consider the symmetric deformation of the regular Kresling origami, which can be defined by the relative rotation $\varphi = \varphi_1 - \varphi_2$ and translation $u = u_1 - u_2$ between the two base polygons, and their circumscribed radii r_1 and r_2. As shown in *SI Appendix*, Fig. S8*A*, we consider the uniform deformation of the rhombic TRP origami, which can be defined by the rotation φ, translation u, and the circumscribed radius r of the base

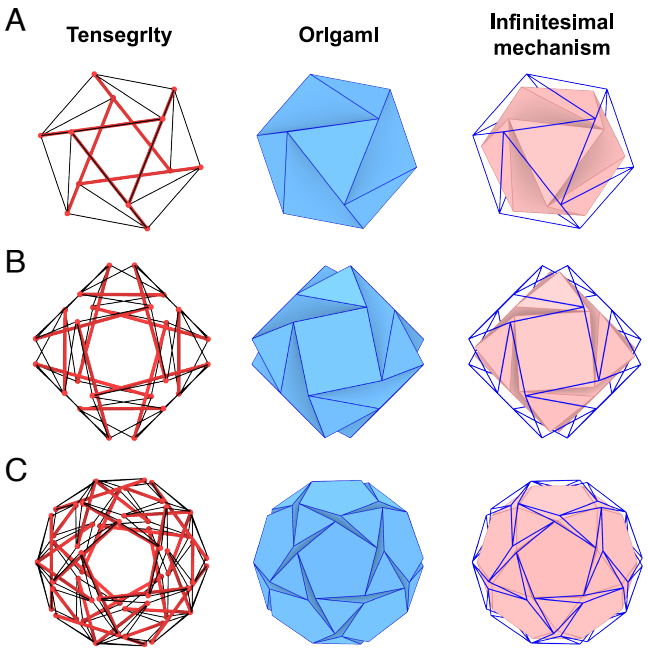

Fig. 7. Rhombic truncated regular polyhedral (TRP) tensegrities (*Left* Column), the dual origami (*Middle* Column), and the infinitesimal mechanisms (*Right* Column). (*A*) The truncated tetrahedral, (*B*) the cubic, and (*C*) the dodecahedral configurations.

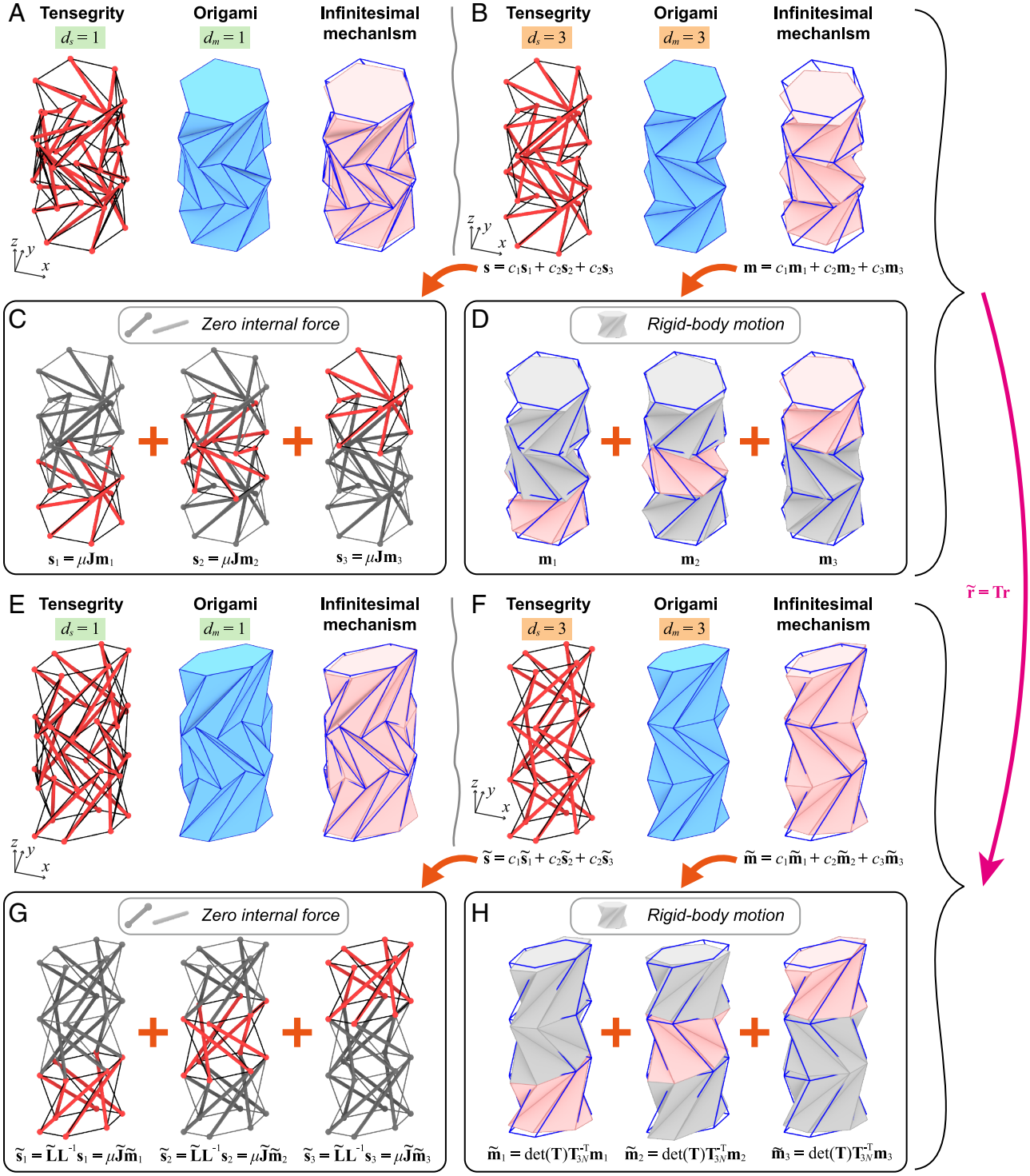

Fig. 8. Three-layer prismatic tensegrities and origami. (*A*) Class-1 and (*B*) class-2 prismatic tensegrities, the dual origami, and the infinitesimal mechanisms ($c_1 = c_2 = c_3 = 1$). (*C*) Three independent states of self-stress $\mathbf{s}_1$, $\mathbf{s}_2$, and $\mathbf{s}_3$ of the class-2 tensegrity. (*D*) Three independent infinitesimal mechanisms $\mathbf{m}_1$, $\mathbf{m}_2$, and $\mathbf{m}_3$ of the dual origami. (*E*) Irregular class-1 and (*F*) irregular class-2 tensegrities, the dual origami, and the infinitesimal mechanisms ($c_1 = c_2 = c_3 = 1$) generated by applying the nondegenerate linear transformation $\mathbf{T}$ to the nodal coordinates $\mathbf{r}$. Here, $\mathbf{T} = \mathbf{S}_{xy}\mathbf{S}_z$, in which $\mathbf{S}_{xy}$ is a simple shear in the *xy*-plane and $\mathbf{S}_z$ is a stretching in the *z*-direction. (*G*) Three independent states of self-stress $\tilde{\mathbf{s}}_1$, $\tilde{\mathbf{s}}_2$, and $\tilde{\mathbf{s}}_3$ of the irregular class-2 tensegrity. (*H*) Three independent infinitesimal mechanisms $\tilde{\mathbf{m}}_1$, $\tilde{\mathbf{m}}_2$, and $\tilde{\mathbf{m}}_3$ of the dual origami.

triangles. In either case, we define the member stiffness as $c_j = EA/\ell_j$, where ℓ_j is the member length and EA is the axial rigidity assumed identical for all the members indexed by j. Then, the deformation energy of these origami is expressed by $U = \sum_{j=1}^{M} c_j(\ell_j' - \ell_j)^2/2$, where ℓ_j' is the deformed member length and U is a function of φ, u, r (or φ, u, r_1, r_2). We consider twist loading so that the constraint forces regarding the translations and radius changes are all zero. Then, based on the principle of minimum potential energy, we minimize U under incremental φ from zero until any face contact (zero dihedral angle) or edge contact (edge-face intersection) occurs. At each loading step (defined by φ), we obtain values of the free variables u and r (or r_1 and r_2). In this way, we obtain the deformation paths of these regular origami structures, including their

nodal displacements $\mathbf{d}_k$, nondimensional deformation energy $U/(EAL)$, and the maximum member strain $|\varepsilon|_{\max}$. Here, L is the length of any valley crease on the undeformed regular origami structures (corresponding to the struts of the dual regular tensegrities). We use the function fmincon in Matlab R2023b to perform the minimization. Once we obtain the nodal displacements $\mathbf{d}_k$ for the regular origami, we use the formula $\tilde{\mathbf{d}}_k = \det(\mathbf{T})\mathbf{T}^{-\mathsf{T}}\mathbf{d}_k$ to approximate the deformation paths of the irregular configurations after the transformation $\mathbf{T}$ and to estimate their $U/(EAL)$ and $|\varepsilon|_{\max}$ (Fig. 4 *B* and *C* and *SI Appendix*, Fig. S13). We note that for the irregular origami, the deformation variable φ is a parameter inheriting from the regular origami and has no direct physical significance.

Fabrication. The tensegrity prototypes (Fig. 2 *A*, *Left* and *B*, *Left*) were fabricated by assembling rigid bars and soft cables. The bars were 3D printed in VeroMagenta using a Stratasys J55 Prime printer. The cables were 3D printed in thermoplastic polyurethane (TPU) using an Ultimaker S7 printer. The origami prototypes (Fig. 2 *A*, *Right* and 2 *B*, *Right*) were fabricated by attaching TANT origami paper pieces with the 3M double-sided tape (9474LE). The paper and tape were cut into desired shapes using a Universal Laser Systems (PLS6.150D) laser cutter. The dimensions of all the components and the assembling guidance are provided in *SI Appendix*, Figs. S14 and S15. The fabricated (undeformed) lengths of the tensegrity bars are considered identical to their assembled (deformed) lengths. For the cables, we roughly assume a uniform elastic strain of 11.1% upon assembly. Accordingly, the fabricated lengths of the cables are set to 90% of their assembled lengths. All cables share the same thickness of 1.5 mm. Under this assumption, the internal forces in the deformed cables are considered proportional to their widths. Since the internal forces in the hexagonal prismatic tensegrities are theoretically proportional to the deformed member lengths (*SI Appendix*, section A), the cable widths are chosen to be proportional to their respective deformed lengths and determined by setting the smallest width to 1.5 mm.

Data, Materials, and Software Availability. All study data are included in the article and/or supporting information.

ACKNOWLEDGMENTS. We acknowledge support from the "Princeton Catalysis Initiative" (PCI) at Princeton University and the National Science Foundation (NSF) under grant 2323276. We thank Kevin T. Liu for insightful discussions.

Author affiliations: [a]Department of Civil and Environmental Engineering, Princeton University, Princeton, NJ 08544; and [b]Princeton Materials Institute, Princeton University, Princeton, NJ 08544

1. C. R. Calladine, Buckminster Fuller's "tensegrity" structures and Clerk Maxwell's rules for the construction of stiff frames. *Int. J. Solids Struct.* **14**, 161–172 (1978).
2. S. Pellegrino, C. R. Calladine, Matrix analysis of statically and kinematically indeterminate frameworks. *Int. J. Solids Struct.* **22**, 409–428 (1986).
3. H. Crapo, W. Whiteley, Statics of frameworks and motions of panel structures: A projective geometric introduction. *Struct. Topol.* **6**, 43–82 (1982).
4. E. D. Demaine, J. O'Rourke, *Geometric Folding Algorithms: Linkages, Origami, Polyhedra* (Cambridge University Press, 2007).
5. T. Tachi, Design of infinitesimally and finitely flexible origami based on reciprocal figures. *J. Geom. Graph.* **16**, 223–234 (2012).
6. B. G. g. Chen, C. D. Santangelo, Branches of triangulated origami near the unfolded state. *Phys. Rev. X* **8**, 011034 (2018).
7. J. McInerney, B. G. g. Chen, L. Theran, C. D. Santangelo, D. Z. Rocklin, Hidden symmetries generate rigid folding mechanisms in periodic origami. *Proc. Natl. Acad. Sci. U.S.A.* **117**, 30252–30259 (2020).
8. R. E. Skelton, M. C. De Oliveira, *Tensegrity Systems* (Springer, 2009).
9. J. Zhang, M. Ohsaki, *Tensegrity Structures* (Springer, 2015).
10. B. S. Gan, *Computational Modeling of Tensegrity Structures* (Springer, 2020).
11. F. Fraternali, J. J. Rimoli, *Tensegrity Systems: Basic Concepts, Mechanical Metamaterials, Biotensegrity* (Springer, 2025).
12. K. Liu, T. Zegard, P. P. Pratapa, G. H. Paulino, Unraveling tensegrity tessellations for metamaterials with tunable stiffness and bandgaps. *J. Mech. Phys. Solids* **131**, 147–166 (2019).
13. D. Misseroni *et al.*, Origami engineering. *Nat. Rev. Methods Primers* **4**, 40 (2024).
14. K. Liu, G. H. Paulino, Nonlinear mechanics of non-rigid origami: An efficient computational approach. *Proc. R. Soc. A Math. Phys. Eng. Sci.* **473**, 20170348 (2017).
15. J. C. Maxwell, XLV. On reciprocal figures and diagrams of forces. *Lond. Edinb. Dublin Philos. Mag. J. Sci.* **27**, 250–261 (1864).
16. N. Watanabe, K. i. Kawaguchi, The method for judging rigid foldability. *Origami* **4**, 165–174 (2009).
17. D. Rus, M. T. Tolley, Design, fabrication and control of origami robots. *Nat. Rev. Mater.* **3**, 101–112 (2018).
18. Z. Zhai, L. Wu, H. Jiang, Mechanical metamaterials based on origami and kirigami. *Appl. Phys. Rev.* **8**, 041319 (2021).
19. M. Johnson *et al.*, Fabricating biomedical origami: A state-of-the-art review. *Int. J. Comput. Assist. Radiol. Surg.* **12**, 2023–2032 (2017).
20. G. M. Scarr, *Biotensegrity: The Structural Basis of Life* (Jessica Kingsley Publishers, ed. 2, 2019).
21. D. S. Shah *et al.*, Tensegrity robotics. *Soft Robot.* **9**, 639–656 (2022).
22. B. Tan, B. Jawed, K. Liu, Tensegrity-inspired sandwich metamaterial for reprogrammable stiffness and impact mitigation. *Int. J. Mech. Sci.* **296**, 110344 (2025).
23. J. Feron, "On tensegrity structures for civil engineering applications," PhD thesis, UCL-Université Catholique de Louvain (2023).
24. K. Liu, G. H. Paulino, Tensegrity topology optimization by force maximization on arbitrary ground structures. *Struct. Multidiscip. Optim.* **59**, 2041–2062 (2019).
25. Y Nishimura, "Static and dynamic analyses of tensegrity structures," PhD thesis, University of California, San Diego, USA (2000).
26. S. Zang, D. Misseroni, T. Zhao, G. H. Paulino, Kresling origami mechanics explained: Experiments and theory. *J. Mech. Phys. Solids* **188**, 105630 (2024).
27. A. Cauchy, Deuxieme memoire sur les polygones et les polydres. *J. de l'école Polytech.* XVIeme cahier, 87–98 (1813).
28. W. Whiteley, "Rigidity of molecular structures: Generic and geometric analysis" in *Rigidity Theory and Applications*, M. F. Thorpe, P. M. Duxbury, Eds. (Kluwer Academic/Plenum Publishers, Dordrecht, Netherlands, 1999), pp. 21–46.
29. W. J. M. Rankine, LVI. On the application of barycentricand projective perspective to the transformation of structures. *Lond. Edinb. Dublin Philos. Mag. J. Sci.* **26**, 387–388 (1863).
30. L. Lu, X. Dang, F. Feng, P. Lv, H. Duan, Conical Kresling origami and its applications to curvature and energy programming. *Proc. R. Soc. A* **478**, 20210712 (2022).
31. R. Connelly, W. J. Whiteley, Global rigidity: The effect of coning. *Discrete Comput. Geom.* **43**, 717–735 (2010).
32. R. Connelly, M. Terrell, Globally rigid symmetric tensegrities. *Struct. Topol.* **21**, 59–78 (1995).
33. A. B. M. Cera, "Design, control, and motion planning of cable-driven flexible tensegrity robots," PhD thesis, UC Berkeley (2020).
34. B. Jessen, Orthogonal icosahedra. *Nord. Matematisk Tidskr.* **15**, 90–96 (1967).
35. L. Y. Zhang, Y. Li, Y. P. Cao, X. Q. Feng, A unified solution for self-equilibrium and super-stability of rhombic truncated regular polyhedral tensegrities. *Int. J. Solids Struct.* **50**, 234–245 (2013).
36. G. Tibert, "Deployable tensegrity structures for space applications," PhD thesis, KTH Royal Institute of Technology, Stockholm, Sweden (2002).
37. C. Qiao *et al.*, Inverse design of kirigami through shape programming of rotating units. *Phys. Rev. Lett.* **134**, 176103 (2025).
38. K. Liu, R. Sun, C. Daraio, Growth rules for irregular architected materials with programmable properties. *Science* **377**, 975–981 (2022).
39. J. Li, "Flexible polyhedra - Exploring finite mechanisms of triangulated polyhedra," PhD thesis, University of Cambridge (2018).